Toward An Empirical Theory of Pulsar Emission. VII. On the Spectral Behavior of Conal Beam Radii and Emission Heights

Dipanjan Mitra

Max-Planck Institut für Radioastronomie, Bonn, Germany; email: dmitra@mpifr-bonn.mpg.de and

Joanna M. Rankin¹

Sterrenkundig Instituut 'Anton Pannekoek', Universiteit van Amsterdam, Amsterdam 1098 EL NETHERLANDS; email: jrankin@astro.uva.nl

ABSTRACT

In this paper we return to the old problem of conal component-pair widths and profile dimensions. Observationally, we consider a set of 10 pulsars with prominent conal component pairs, for which well measured profiles exist over the largest frequency range now possible. Apart from some tendency to narrow at high frequency, the conal components exhibit almost constant widths. We use all three profile measures, the component separation as well as the outside half-power and 10% widths, to determine conal beam radii, which are the focus of our subsequent analysis. These radii at different frequencies are well fitted by a relationship introduced by Thorsett (1991), but the resulting parameters are highly correlated. Three different types of behavior are found: one group of stars exhibits a continuous variation of beam radius which can be extrapolated down to the stellar surface along the "last open field lines"; a second group exhibits beam radii which asymptotically approach a minimum high frequency value that is 3-5 times larger; and a third set shows almost no spectral change in beam radius at all. The first two behaviors are associated with outer-cone component pairs; whereas the constant separation appears to reflect inner-cone emission. The first group, remarkably, can be fitted by a Thorsett relation in which the constant term is constrained to be the field-tangent direction at the edge of the polar cap $\rho_{\rm pc}$, but the others cannot. The first group can also be fitted well using an index of -1/3, but the second group cannot.

We first compute heights from the conal beam radii, assuming dipolar fields and emission along the "last open field lines"—which we find are again well fitted by a suitable Thorsett relation. Here we find that the first group can be fitted using a constant term $h_{\rm pc}$ of 10 km and also that the first two groups are remarkably well fitted by an index of -2/3. We then argue that physical emission heights can be estimated using the component separation along an interior annulus of field lines having their "feet" about halfway out on the polar cap—and such values agree well with most existing height values based on physical criteria.

Therefore, we find that "radius-to-frequency" mapping is associated with outer-conal component pairs. The near constant behavior of inner-cones is thus arresting. We explore possible interrelationships between the spectral behavior of the component and profile widths produced both by the field-line flaring and the changing sightline geometry. We also attempt to understand the physical implications of the parameter values resulting from the Thorsett-relation fits.

Subject headings: MHD — plasmas — pulsars: general — pulsars: individual (B0301+19, B0329+43, B0525+21, B0834+06, B1133+16, B1237+25, B1604+00, B1919+21, B2020+28, B2045-16) — radiation mechanism: nonthermal

1. Introduction

Those few bright, relatively local pulsars exhibiting a well resolved pair of conal components have had major influence on our conception of pulsar radio emission. They represent only a handful of the 1000+ stars now known, and some of their original "B" designations come easily to the tongue: B0301+19, B0329+54, B0525+21, B1133+16, B1237+25, B2020+28, and B2045-16, having each been the subject of sundry studies over the years. This small group comprises the finest examples of stars exhibiting a monotonic increase of total profile width, or conal componentpair spacing, with wavelength. Such behavior, noted in the earliest efforts to systematize and understand pulsar radio emission (e.g. Komesaroff 1970, Komesaroff, Morris & Cooke 1970, Lyne, Smith & Graham 1970; Sieber, Reinecke & Wielebinski 1975; Cordes 1978), has generally been regarded as primary evidence that the lower frequency radio emission is emitted at higher altitudes in the pulsar magnetosphere. While this phenomenon, known as "radius-to-frequency mapping" (hereafter RFM), is clearly exhibited by many pulsars, it is particularly marked in lower frequency (f < 100 MHz) observations. quently, it is only a few local (low dispersion) objects that can be observed over the 8–10-octave frequency range needed to examine its character in adequate detail.

Thorsett (1991) nicely summarizes the early history of the RFM discussion: Observationally, it rapidly became clear that no simple curve fitted the measurements, so that the component-pair width (or separation) behavior (as longitude intervals $\Delta \varphi$, 360° corresponding to one rotation period P) was usually described by fitting powerlaw functions f^{-a} to the asymptotic high and low frequency values. Theorists, meanwhile, began to predict various dependences for the RFM—the height proportional to $f^{-2/3}$ relation encountered in models where the characteristic emission frequency is equated to the plasma frequency (such as for curvature radiation)—being the most often encountered. Later studies suggested that the index a varied continuously with frequency (i.e. Rankin 1983b; hereafter Paper II) and, therefore, that no single power-law relation could describe the overall behavior (Slee, Bobra & Alurkar 1987). Thorsett then evaluated two simple generalizations of a single power-law

$$\Delta \varphi = (f/f_o)^a + \Delta \varphi_{\min}, \text{ and } (1)$$

$$(\Delta\varphi)^2 = (f/f_o)^a + (\Delta\varphi_{\min})^2, \tag{2}$$

(where f is the radio frequency) and found that they fitted his measurements equally well.

Over this same period, ideas developed regarding the geometrical significance of these prominent component pairs. First, they were demonstrably conal—that is, they represented a relatively central sightline traverse through a hollow-conical emission pattern (Rankin 1983a; hereafter Paper I). Second, the magnetic latitude α and sightline impact angle β could be estimated by various techniques (e.g. Lyne & Manchester 1988), taking the polarization-angle (hereafter PA) sweep rate R to be $|\sin \alpha / \sin \beta|$ (Radhakrishnan & Cooke 1969; Komesaroff 1970). And third, these conal beam radii assumed particular dimensions in terms of the polar cap radius, which in turn suggested specific emission heights (Rankin 1993a,b; hereafter Paper VIa,b).

Surprisingly, few attempts have been made to amalgamate these discussions, to the end that questions relating to the frequency dependence of width (or separation) can be explored in the context of a specific emission geometry. Two such attempts are those of Xilouris et al (1996) and von Hoensbroech & Xilouris (1997b) which we will discuss further below. Clearly, a much more appropriate quantity with which to assess the RFM is the conal beam radius ρ (which has primary geometrical significance; see Paper VIa: fig. 2), rather than the various observed intervals of longitude $\Delta \varphi$ (which conflate the accidental geometry of the observer's sightline). Moreover, once $\rho = \rho(f)$ has been determined, the emission height h can easily be estimated (assuming a dipolar magnetic field geometry), so that the RFM can be assessed directly as a frequency-dependent height relation h=h(f). Our purpose in the remainder of this paper is then a) to combine measurements used by Thorsett with more recent and accurate profile observations, b) to study their implications in the context of an appropriate geometrical model, and

¹On leave from the Physics Department, University of Vermont, Burlington, VT 05405 USA; email: rankin@physics.uvm.edu

c) to draw what physical conclusions we can from the results of these analyses.

2. Measurements and Analysis

Table 1 gives parameters of the pulsars which are the subjects of this analysis—that is, two groups comprising the seven primary stars already mentioned as well as three others—which will be discussed as needed below. Our profile measurements were taken both from those sources identified by Thorsett (see his Table I and the references therein) and from more recent published and unpublished work. These additional sources are listed below Table 2 and include high quality Arecibo observations at between 25 MHz and 6 cm (Hankins, Rankin & Eilek 2002).

The various observations were reduced to sets of profile measurements using a combination of handscaling and, where appropriate, fitting Gaussian functions to the relevant components (see Kramer 1994; Kramer et al 1994). In all cases we were interested in a) the half-power (3-db) widths of the respective components, b) the separations between the centers of the component pairs, c) the full profile widths at the outside half- and 1/10power points, and d) reasonable error estimates of these values. In practice the outside half-power (3db) points were determined separately for the two components as their amplitudes were usually different (see Backer 1976; figs. 2c,d). Generally, we found the fitting more useful to locate the component centers for the separation measurements, but in many cases the 3-db profile widths could also be accurately estimated by summing the componentpair separation and half the sum of their fitted widths. As can be seen in the following plots and tables, it was usually possible to estimate a given quantity in several different ways (including making use of Thorsett's independent values), so that there is a good deal of redundancy in our measure

The errors in the widths $\sigma_{\Delta\varphi}$ were estimated wherever possible by using the formal errors of the Gaussian fits, which it turn were based on well determined values of the noise in the off-pulse region of the profile. Where hand-scaling was used, the errors were again estimated from the quality of the profile and the off-pulse rms-noise level.

3. Component-Width Spectra

Most previous attempts to understand how the widths of profile components vary with frequency have only proved frustrating. Until the last decade or so, no pulsar's profiles were well enough measured—particularly at low frequency—that this important issue could be addressed with any confidence. As the brightest star in the sky with two well resolved profile components, pulsar B1133+16 ostensibly offers the best possible context for studying its component-width behavior, but Rankin's (Paper II) effort to draw conclusions from the then available profile data (see her fig. 5), we will now see, was inconclusive and misleading in its suggestion of a monotonic increase of width with wavelength—though Izvekova et al (1993), a decade later, were able to discern a nearly invariant behavior over a narrower frequency range.

The lower portion of Figure 1 gives a pair of component-width spectra for B1133+16, where the values for the leading (I: asterisks) and trailing (II: circles) components are plotted according to the "Component Width" scale. While these width values are hardly constant, they do not begin to mimic the monotonically varying profile-width curves in the upper part of the figure. Though we see discrepancies among the well measured values (e.g., around 400 MHz), most of the values are roughly compatible, within their errors, with a constant width at frequencies above about 40 MHz: $2.2^{\circ}\pm0.6^{\circ}$ and $3.2^{\circ}\pm0.9^{\circ}$ for components I and II, respectively. Only below 40 MHz and around or above 3 GHz do the component-widths diverge from these values.

Further, the increases below 50 MHz appear to be just what might be expected from instrumental effects. Scattering broadening also becomes important for these low dispersion measure DM objects at low frequencies, but it is usually quite clear when it is the dominant effect, because of its steep $f^{\sim -4.4}$ dependence. At the lowest frequencies the necessarily narrow filter bandwidths Δf entail risetimes which become comparable to the dispersion smearing—so that the minimum achievable (non-coherently dedispersed) resolution escalates as $f^{-3/2}$. If the filter risetime Δt_r is of the order of $2\pi k/\Delta f$ (where k is a small positive value), and the dispersion smearing Δt_d goes as $DM\Delta f/f^3$, then for optimum choices of parame-

Table 1
Pulsar Parameters.

Pulsar (B-)	Period (s)	DM (pc cm ⁻ 3)	$f_{1^{\circ}}$ (MHz)	B ₁₂ (G)	α (°)	R	β/ρ [at 1GHz]
0301+19 $0525+21$ $1237+25$ $2045-16$	1.388 3.745 1.382 1.962	15.69 50.87 9.28 11.51	41 42 47 40	2.7 24.6 2.34 9.34	38 ± 5 21 ± 2 53 ± 3 34 ± 2	17 ± 1 36 ± 1 ∞ ? 30 ± 2	0.45 0.19 ~ 0 0.26
0329+54 $1133+16$ $2020+28$	0.715 1.188 0.343	26.78 4.85 24.6	103 41 164	2.46 4.26 1.62	32 ± 3 46 ± 3 56 ± 5	10 ± 3 10 ± 1 6 ± 1	$0.31 \\ 0.78 \\ 0.49$
0834+06 $1604-00$ $1919+21$	$ \begin{array}{c} 1.274 \\ 0.422 \\ 1.337 \end{array} $	12.86 10.72 12.43	55 108 53	$5.9 \\ 0.72 \\ 2.7$	30 ± 6 50 ± 5 34 ± 3	9 ± 2 8 ± 2 11 ± 2	$0.86 \\ 0.82 \\ 0.76$

ters $\Delta t_{\rm min}$ (= $\Delta t_r = \Delta t_d$), we find that $\Delta t_{\rm min}$ (°) is about 145°[$kDM/P^2({\rm s})$]^{1/2}f(MHz)^{-3/2}. Table 1 gives the frequencies $f_{1^{\circ}}$ at which this limiting resolution represents a longitude of 1° (for k=1). Were then k very reasonably some 2–4, we can understand the width escalation for 1133+16 at and below 50 MHz as instrumental in origin. We have thus corrected the low frequency width values for this limited resolution (taking k to be about 3) on the plots and in our subsequent analyses.

The lower curves of the plots in Figure 2 give component-width spectra for six additional stars, exactly as did the B1133+16 plot in Fig. 1. Apart from the strange "step" in B0301+19, we see a relatively constant component-width behavior. No pulsar exhibits a width escalation with wavelength which at all mimics the corresponding profile behavior in the upper panels. In order to further understand the frequency dependence of the component widths, we fitted power-law curves of the form Kf^{ζ} , where f is in GHz. Table 2 then gives the resulting parameters over (in some cases) several ranges of frequency. Most of the stars have one component—and both for B0525+21 and B1237+25—which exhibits and an essentially constant width within the errors. Only for B2045– 16 do we see a clear spectral trend for both components—or, in other words, where ζ appears significant. More often, the widths are "noisy", varying somewhat both at a given frequency and

unsystematically over the entire observed band.

We can see that even with our corrections, some of the lowest frequency values remain anomalously large. It is possible that scattering becomes a factor, but more likely these lowest frequency profiles are "smeared" by unknown instrumental factors which are not completely correctable. Therefore, only when future coherently dedispersed observations at very low frequencies become available can we interpret them with full confidence.

We see no evidence for the leading or trailing component to be larger. There may be some tendency for the components to narrow at the highest frequencies—perhaps resulting in the largest widths in the mid-frequency range. Though this trend hardly significant for any particular star (perhaps for B2020+28), we find the very smallest widths in the extreme high frequency profiles in about half of the cases (see also fig. 3).

In considering the width variations, it is also very possible that one or both of the two components are composite, with modal contributions that may have somewhat different temporal and spectral behaviors. Indeed, there is now increasing evidence that these conal components are comprised of modal contributions which have somewhat different angular dependences (see, for instance, Rankin et al 1988; Ramachandran et al 2002; as well as Paper VIII in this series), and

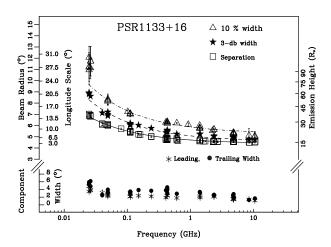


Fig. 1.— Component-pair widths (lower portion), 10\% and 3-db profile widths, and component separations (upper portion) for pulsar B1133+16 as a function of frequency. The component and profile widths have been corrected for the estimated low frequency instrumental broadening (see text), significant here only at 25 MHz where it has reduced the plotted values by around 1°. The three profile measures are plotted according to three separate scales: longitude (inside left), inferred beam radius (outside left), and inferred emission height (outside right); note that the first and last scales are necessarily somewhat non-linear. Keys to the respective symbols are given on the plot. The respective curves, fitted both to the conal beam radii and component widths, are discussed in the text.

were these to overlap increasingly in the often somewhat narrower high frequency components, it could account for the progressive average depolarization that characteristically occurs there (e.g. McKinnon 1997).

We have entertained whether the cases of possible high frequency component narrowing might be associated with "breaks" in the radiofrequency spectra for these stars. Such features have been identified in the spectra of B0301+19 (0.9 GHz), B0525+21 (1.5 GHz), B1133+16 (2.0 GHz), B1237+25 (0.7 GHz), B2020+28 (2.3 GHz) and B2045-16 (0.5 GHz) (Malofeev 1994, 2001; Maron et al 2000; McKinnon 1997). For all but the second, the turndown frequencies seem roughly compatible with their width spectra, but more careful work will be required to fully demonstrate this association.

We conclude that these well measured component widths are virtually constant with frequency, apart from a slight tendency to narrow at high (>1 GHz) frequencies.

4. Conal Beam Radii

As mentioned earlier, the conal beam radius ρ is a far more appropriate quantity by which to assess RFM questions, as it is a fundamental descriptor of a star's emission geometry. If we assume a *circular* emission beam, then when the magnetic latitude α and sightline impact angle β are known, we can compute ρ using the spherical geometry relation first given by Gil (1981)

$$\sin^2 \rho / 2 = \sin \xi \sin \alpha \sin^2 \Delta \varphi / 4 + \sin^2 \beta / 2, \quad (3)$$

where $\xi=\alpha+\beta$. α can be estimated either using the techniques of Lyne & Manchester (1988) or the core-component-width method of Paper IV, wherein the 1-GHz core width W_c is $2.45^{\circ}P^{-1/2}/\sin\alpha$. Fortunately, for the three stars here with core components, the two methods agree very closely. Pulsars B0301+19, B0525+21, B1133+16 and B2020+28 have no detectable core components and thus the second method cannot be used to determine α . However, Paper VI found that cones have definite angular dimensions in terms of the polar cap radius, and these four pulsars all seem to have what were called "outer" cones with 1-GHz, half-power radii of 5.75° $P^{-1/2}$. So here we can work backwards, given a particular

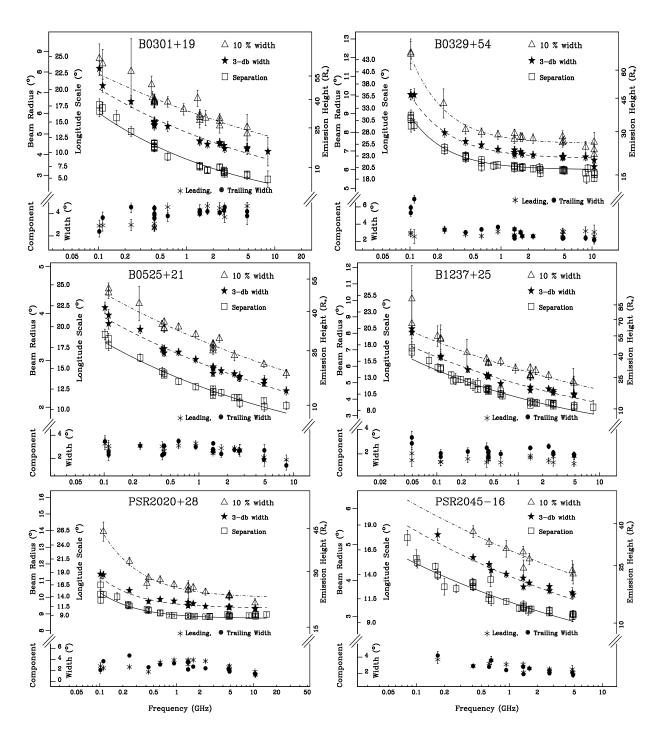


Fig. 2.— Component-pair widths (lower portion), 10% and 3-db profile widths, and component separations (upper portion) for pulsars B0301+19, B0329+54, B1133+16, B1237+25, B2020+28, and B2045-16 as Fig. 1.

conal type, by then finding the value of α which squares with the characteristic 1-GHz value of ρ .²

Secondly, we estimate the impact angle β as $\sin \beta = \sin \alpha/R$, where $R \ (=|\partial PA/\partial \varphi|_{max})$ is the maximum sweep rate. Table 1 lists the values of α , R and β/ρ (at 1 GHz) as taken from Paper VI. As we do not know the sign of β for any of the stars of interest here, we have proceeded as if β could be of either sign—and the difference affects our results so little that it has been accommodated within the stated errors.

Assuming that β , ρ and $\Delta \varphi$ are small and independent, the error σ_{ρ} in ρ can be calculated by propagating the errors σ_{α} , $\sigma_{\Delta\theta}$, and σ_{R} (given in Table 1) as,

$$\sigma_{\rho}^{2} = A_{\alpha}(1 + \Delta\theta^{2})\sigma_{\alpha}^{2} + A_{\Delta\theta}\sigma_{\Delta\theta}^{2} + A_{R}\sigma_{R}^{2}$$
 (4)

where $A_{\alpha} = (\sin \alpha \cos \alpha/4\rho)^2$, $A_{\Delta\theta} = (\Delta\theta \sin^2 \alpha/4\rho)^2$, and $A_R = (\sin^2 \alpha/2R^2\rho^2)^2$.

With these considerations in mind we can now compute ρ and σ_{ρ} from α , R and $\Delta \varphi$. We wish to fit the resulting ρ values in order to study their frequency variation, but we have no a priori means of knowing how they will behave—or in our practical terms, what an appropriate fitting function might be. However, for some pulsars (with small β/ρ , such as B1237+25), we know that the ρ and $\Delta \varphi$ behavior cannot be very different, so that a "recycled" empirical Thorsett expression may well serve adequately for the ρ fitting also—

$$\rho = \rho_{\circ} + (f/f_{\circ})^a, \tag{5}$$

where ρ_{\circ} and f_{\circ} are constants in degrees and degrees-GHz^{-a}, respectively.

The upper portions of Figures 1 and 2 give the respective measured values, along with their errors, for the component separation, outside half-power (3-db) profile width, and the outside 10% width of the seven primary stars in consideration. Note that these primary data are plotted according to the slightly non-linear longitude scale on the inside, upper left of the diagrams. The computed conal beam radii are then plotted per the

linear "Beam Radius" scale on the outside, upper left of the plots. These three primary measures, of course, refer to somewhat different positions on the conal emission beam (as well as incurring slightly different geometrical factors), and so they may or may not behave similarly when fitted.

In order to carry out the non-linear leastsquare-error analysis, we used the Levenberg-Marquardt method as implemented in the Numerical Recipes routines (Press et al 1986), fitting all three profile measures: separations, half-power widths, and 10% widths. We first tried unconstrained, 3-parameter fits and found that while the Thorsett expression fitted the profile measurements adequately—that is, with χ^2 values near unity—the parameters were all highly correlated. Table 3 summarizes the fitted parameters, normalized correlation coefficients, reduced χ^2 values, and number of fitted points M, for some of these fits. The correlations between ρ_{\circ} and f_{\circ} ran between +0.74 and +0.93, those between f_{\circ} and a around -0.98, and the third one also negative and intermediate in magnitude.

In an effort to provide some physical constraint on the fitting function, we attempted to interpret ρ_{\circ} , the infinite-frequency value of ρ , in terms of the field direction at polar cap edge $\rho_{\rm pc}=1.23^{\circ}P^{-1/2}$. This $\rho_{\rm pc}$ is associated with the "last open field lines" and may or may not represent the radius of the "active" region on the stellar surface, but it seemed meaningful to ask whether such a small asymptotic value could be compatible with the overall frequency dependence of the conal beam radius. Moreover, we do not know which profile measure, if any, might correspond to this outer boundary of the polar cap. Therefore, we explored the behavior of all three.

It was thus surprising to find that upon fixing ρ_o as $\rho_{\rm pc}$, very adequate fits were obtained for four stars, B0301+19, B0525+21, B1237+25 and B2045-16 (hereafter Group A). The results are given at or near the top of each section in Table 3—with the fixed ρ_o values shown in boldface—and the three respective fits for each pulsar are hardly better in one case or the other as judged by the χ^2 values. It thus seems that the A-group stars are insensitive to assumptions about what point on their profiles corresponds to the "last open field lines". The A-group f_o values are well beyond the highest frequency observa-

²Weak arguments were used to classify pulsar B2020+28 as an inner-cone **T** star in Paper VI, and viewing it as an outer conal double (**D**) object also raises problems. Its PA traverse departs significantly from the usual "S" shape, so its R of >10 may not have the usual significance. α must be nearly 90° if R is as large as 8. We used the somewhat smaller values in Table 1.

tions, reflecting the fact that it is only here that the second term in eq.(5) declines to a value of 1°. Qualitatively, we see this behavior clearly in Figs. 1 and 2 as the A-group measures continue to decrease at the highest frequencies (in marked contrast to the remaining stars, which approach an asymptotic width at high frequency).

Then, we asked whether reasonable fits for the A-group stars could be obtained if ρ_{\circ} was fixed as above and the index a was set to the (plasma frequency associated) value of -1/3—and the answer was negative. We give these fitting results only in terms of the component separation, and the corresponding entries in Table 3 show that the χ^2 values fall far above unity. Finally, we asked whether fixing a at -1/3 was compatible with the observations if the constraint on ρ_{\circ} was relaxed, and our results for the separation measure appear just under the foregoing ones. Again, to our surprise, we found that these fits were very acceptable (slightly better than those obtained by constraining ρ_{\circ}), with values of ρ_{\circ} well larger than $\rho_{\rm pc}$ by factors of between 3/2 and 3.

However a similar exercise for PSRs B0329+54, B1133+16 and B2020+28 (hereafter Group B) shows a very different behavior. The first group of (separation) results quoted for these stars in Table 3 represents the unconstrained fits. For these stars, the parameters are slightly better determined as ρ_{\circ} and f_{\circ} are only about 80% correlated. This is so because here the ρ values saturate rather rapidly with frequency—i.e. at 300 MHz or so—as can be seen by the very different f_{\circ} values for the B-group stars. Again, apart from the halfpower width fit for B1133+16 (where $\chi^2 \sim 4$), the profile measure has very little effect on the fitting quality.

As might be expected from the qualitative behavior, no acceptable fits could be obtained for the B-group stars when $\rho_{\rm o}$ was constrained to $\rho_{\rm pc}$. When the index a was fixed at -1/3 as above though, Table 3 shows that all the χ^2 s fall just above the acceptable range. Moreover, the $\rho_{\rm o}$ values are all about 3 times greater than $\rho_{\rm pc}$, just as for the A-group stars. The $f_{\rm o}$ values remain low, 2–10 times those for the free fits, and representing frequencies within the range observed.

Summarizing then, conal beam radii computed from the three profile measures are well fitted by eq.(5) with unconstrained parameters, though with very high correlations. Only for the A group, however, do acceptable fits obtain when ρ_{\circ} is fixed at $\rho_{\rm pc}$ or a to -1/3.

5. Do Inner Cones Exhibit RFM?

Figure 3 gives similar displays for three additional pulsars, B0834+06, B1604-00 and B1919+21. All exhibit a very different behavior—a near constancy of their profile dimensions. Sieber et al's (1975) study found, for B0834+06 and B1919+21, a slight width escalation both above and below about 200 MHz, trends which can be seen in our plots as well. Of course, this behavior does not permit fitting eq.(5) to the profile measures, so instead we plot lines showing the best-fitting constant values. Overall, the separation is virtually fixed for these objects within their errors. The profile width measures show somewhat more variation, in part reflecting changes in the component widths, which tend to be largest at intermediate frequencies. The one-parameter fitting results for these stars are given in Table 3 as Group C.

The ostensible complete lack of RFM in these Group C stars is so striking in contrast to the foregoing A- and B-group pulsars that it demands further inquiry. A hint comes from B1604–00, whose triple **T** profile's core-component width can be determined accurately (Rankin 1986), and modeling its emission geometry (Paper VI) indicates that its conal component pair represents an inner cone. The star's three primary components overlap, but they can be segregated either polarimetrically or by Gaussian fitting. Here the high quality Arecibo profiles of Hankins et al (2002) have been especially useful.

No core component has been identified in the other two group-C pulsars, so it is not possible to be as definite about their geometry; however, the overall structure of both could well be of the innercone type. Pulsar B0834+06 was analyzed as having an inner cone in Paper VI; whereas the complexity of B1919+21's emission (e.g., Prósynski & Wolszczan 1986) then tended to suggest a double-cone structure—in turn then implying an outer cone—but with recent evidence for one smaller "further-in" cone (Gil et al 1993; Rankin & Rathnasree 1997; Gangadhara & Gupta 2001; hereafter G&G), B1919+21's conal structure could still be

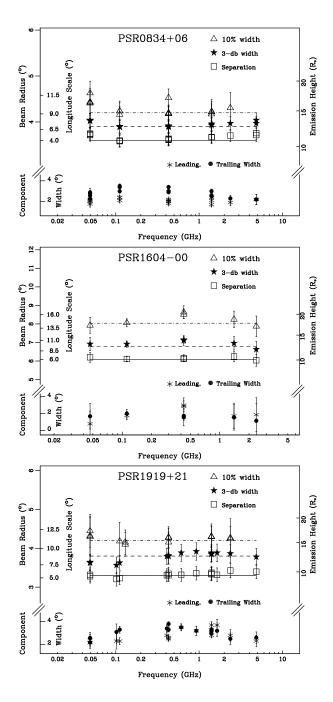


Fig. 3.— Component-pair widths (lower portion), 10% and 3-db profile widths, and component separations (upper portion) for pulsars B0834+06, B1604-00 and B1919+21 as Fig. 1. Note that these stars exhibit almost no change in their component separations and very little in their profile widths.

of the inner type.³

Interestingly, the width spectra of these three stars—with demonstrated or probable inner-cone configurations—have very much in common with what is known about the inner cone behavior in the double-cone, five-component M pulsars that were studied in Paper VI. Unfortunately, only three, B1237+25, B1451-68 and B1857-26, have been studied sufficiently well over a wide enough frequency range to give even a qualitative indication of inner-cone separation spectra. These data are tabulated in Paper VI, Table 3, and for the first two stars it can be seen that the inner cone, halfpower pair widths are either nearly constant or much more slowly varying than the corresponding outer conal pair. For B1857-26, the existing observations provide only the qualitative impression that the inner cone dimensions remain relatively $constant.^4$

So, in short, if the primary conal component pairs in these stars are inner cones, then perhaps this highly unusual emission on the fringes of their profiles should be interpreted as evidence for weak outer-cone emission. It is worth noting that these three pulsars are some of the strongest and least dispersed in the sky, so we have a much greater opportunity to obtain sensitive profiles wherein low level emission could be detected over a wider frequency range (including on an individual-pulse basis). Conversely, the Group A and B stars are at least equally bright and little dispersed, and we see nothing of this weak outlying emission in these stars.

All three group-C stars deserve major new observational and analytical attention: Two are Cambridge pulsars which have had very little recent study. All would benefit from the single-pulse polarimetry techniques developed since the 1990s, carried out over a wide frequency range.

³Additionally, the three pulsars share a further unusual characteristic: their profiles exhibit low level emission well outside the two main conal features, particularly on their leading edges. In B0834+06 this can be seen very clearly in the recent work of Weisberg et al (1999), but other observations also show a "ramp" or weak leading-edge feature (e.g. Kardashev et al 1986). In B1604-00's profile the early emission is very prominent. Weisberg et al's profile clearly shows the inflections corresponding to the core and two conal features as well as marked emission well before them. Finally, we see a very similar behavior in B1919+21; the profiles in Hankins et al (2002), Gould & Lyne (1998), and Weisberg et al (1999) all show a leading-edge feature which appears to be strongest at very low and high frequency—and some suggest similarly enhanced emission on the trailing edge also. In fact, in the 4.85-GHz profile in von Hoensbroech's (1999) thesis, this emission appears as a distinct preceding component.

⁴Again, much more work is needed to elucidate not only the behavior of these three "exemplars" but also the many other and/or more recently discovered M pulsars.

One additional means of attempting to confirm this striking lack of RFM in inner conal component pairs is that of examining the behavior of other stars, like B1604–00, with innercone triple **T** profiles. We found in Paper VI that about half the **T** stars had inner cones (23) of 40), and recent observations—particularly by Gould & Lyne (1998; hereafter G&L)—now provide good quality profiles over a wide enough band (1642 to 234 MHz) to see if their conal configurations change very much. A full analysis of this question goes beyond the scope of this paper, because most of the inner cone T stars will require fitting to accurately locate their components. However, we can get a useful qualitative impression. Of the 22 pulsars apart from B1604-00 (and using G&L, Hankins et al 2002, and the sources in Paper VI), 13 stars, B0149-16, B0450+55, B0450-18, B0919+06, B1221-63, B1508+55, B1541+09, B1702-19m, B1706-16, B1727-47, B1747-46, B1818-04, and B1839+09, have profiles in which the inner-conal pair spacing changes hardly at all. Further, none of the 9 others provides a contrary example (most have not been observed at low enough frequency, are scattered, or are simply too weak to bear on the question).

The conclusion then seems inescapable: the conal beams comprised by inner cones exhibit virtually no RFM—that is, inner conal component pairs show little or no change in their longitude separation—in turn implying that the inner conal beams which produce them have radii that vary little or hardly at all with frequency. The RFM behavior of the outer cones of Groups A and B and the inner cones of Group C (and the other stars mentioned above) could hardly be more different. The former exhibit the rather dramatic RFM which has attracted the attention of many investigators; whereas, the ostensibly similar inner cones (differing only in their distinct characteristic angular size relative to that of the polar cap $\rho_{\rm pc}$) show no discernible RFM at all.

6. Reconciling the Conal Beam Measures

Let us now compare the results of the above analysis with the earlier published work on conal beam dimensions. We mentioned above the conclusion (Paper VI) that most conal beams have two characteristic outside, half-power radii, $\rho_{\rm inner[outer]} = 4.33^{\circ}[5.75^{\circ}]P^{-1/2}$ at 1 GHz. In addition, there are further results from Gil et al (1993), Kramer et al (1994), Rankin & Rathnasree (1997), Mitra & Deshpande (1999), and Gangadhara & Gupta (2001). In analyzing their profile-dimension information, these authors used different measures, and now, using our analysis tools, we can find a relationship between them.

We have seen above that the various measures fit the respective profiles with somewhat different parameters. However, the largest part of this difference is in the very different spectral behavior of the 3-db and 10% component widths. As these widths are fairly constant, very similar values for f_{\circ} and a should be obtained in fitting any of the three profile measures; the difference will appear almost entirely in ρ_{\circ} . Therefore, we proceed here by imposing values of f_{\circ} and a, obtained from fitting the separations, on the profile-width fits in order to study their relationship.

Specifically, for the A-group pulsars, we imposed f_{\circ} and a values, obtained from the $\rho_{\circ} = \rho_{pc}$ constrained, component-separation fits in order to obtain the best fitting values of ρ_o , $\rho_{cs} = \rho_{pc}$, ρ_{3db} , and $\rho_{10\%}$. We computed $\rho_{3\text{db}} - \rho_{\text{cs}}$ and $\rho_{10\%} - \rho_{\text{cs}}$ for each star, and found that the ratios were in reasonable agreement, yielding an average value of 0.51 ± 0.15 . Therefore, the 10% point on the conal beam seems to fall twice as far from the peak as from the half-power point. A similar ratio can be gleaned from the results of Gil et al (1993), whose ensemble 3-db and 10% points fall at $5.52^{\circ}\pm0.5^{\circ}$ and $6.33^{\circ}\pm0.5^{\circ}$, respectively, in relation to a peak value at 4.6°. This dependence is not far from that of a Gaussian curve, where the half-power point falls at 0.55 that of the 10% point.

A similar procedure was carried out on the Group B and C stars (without the $\rho_{\circ}=\rho_{\rm pc}$ constraint). For the B group, the component-separation fit values can be imposed on the other two measures only if some high and low frequency values are omitted (because of changes in the component widths), and for the C group only an overall ρ_{\circ} can be defined. The average values of the ratios was thus 0.42 ± 0.1 and 0.45 ± 0.1 for Group B and C, respectively—slightly lower perhaps than for the Gaussian curve.

Overall then, we conclude that conal beams have a roughly Gaussian dependence in ρ .

7. Emission Height vs. Frequency

We now consider the implied heights of emission, assuming first a dipole structure for the stellar magnetic field, and second that the emission at a given frequency arises from the same altitude above the center of the 10-km neutron star. The radio emission height h can thus be computed as

$$h = 10P(\rho/1.23^{\circ})^2 \text{ km}.$$
 (6)

Then, since ρ is a function of frequency as given by the neo-Thorsett relation eq. (5), the dependence of h on frequency—RFM mapping—can be studied directly. The upper portions of all the foregoing figures show this computation of h on their outside, right-hand scales in units of the (putative 10-km) stellar radius R_* . Because our analysis used values of α and β estimated by one of us (Paper VI)—which in turn used the convention of associating the emission with the "last open field lines"—the 1-GHz, 3-db-width heights for the group A and B stars (all shown or thought to be outer cones) in these figures are all just over 200 km. The heights corresponding to the separation and 10% widths are consequently smaller and larger, respectively.

It is certainly possible to relate the fitting data in terms of ρ [eq.(5)] to the height expression above. In that $h \propto \rho^2$, the fitting function must be squared, and the uncertain effect of the cross term complicates interpretation. A more transparent approach is that of fitting the frequency dependence of h directly. In that we have no a priori knowledge of h=h(f), we want to assess this approach to ensure that our results are meaningful. Again, we try a version of Thorsett's relation

$$h = h_{\circ} + (f/f_h)^b, \tag{7}$$

where h_{\circ} and f_h are constants in units of km and GHz-km^{-1/b}, respectively.

In order to fit eq.(7) we used the separation measure, as use of the others would lead to similar results, while raising the complications discussed above. The results of the fits are summarized in Table 4. The fitting procedure was identical to that for eq.(5) above. Once again, the unconstrained, 3-parameter fits are presented first for both the group A and B stars, and both give uniformly good χ^2 values.

In an effort to understand our earlier fitting results for $\rho = \rho(f)$, we attempted to test the situation where h_{\circ} is fixed to R_{*} (corresponding to $\rho = \rho_{\rm pc}$) and the index b = 2a—obtaining unsatisfactory fits (not shown) for both the A and B groups ($\chi^{2} \sim 200$ for the latter). However, the middle set of A-group results shows that decent fits do obtain with h_{\circ} set to R_{*} , but with b values somewhat different than 2a.

Then we asked if reasonable fits are obtained if h_{\circ} is constrained to R_{*} and b to the plasma-frequency-associated value of -2/3, and again the answer was negative for both groups. However, if h_{\circ} remains unconstrained, very reasonable fits are obtained for all the A-group stars as reported in Table 4, though the resulting h_{\circ} values are 5–10 times larger than R_{*} . In comparing these results with the heights inferred from the corresponding ρ_{\circ} values in Table 3 where a=-1/3, we find that the latter are only slightly smaller—suggesting that the overall effect of the cross-term is small.

Finally, we turn to the B group and carry out the same fitting procedure, first freeing all three parameters and then fixing only b at -2/3. Surprisingly, reasonable fits were obtained in both cases, the former having only slightly lower values of χ^2 as shown in Table 4. Recall that when group B fits were made for ρ in Table 3, holding $a{=}-1/3$, the results were were rather poor.

It is indeed remarkable that by fitting h=h(f) directly using eq.(7), both the A- and B-group stars exhibit a consistent behaviour with the index b=-2/3 and with f_{\circ} values falling in a relatively narrow range between about 50 and 150 km. These fits suggest that only an index value near -2/3 could accommodate the different characteristics of the A and B groups.

8. More Physical Height Estimates

The height estimates made by one of us in Paper VI are in need of revision. The convention there of associating the outside 3-db points of the component pairs with the full polar cap radius (or the "last open field lines") is not very physical, first because the electric field **E** is expected to vanish along this boundary and second because we are interested in the effective height of the emission region, not its lower edge.

A better convention, we now believe, is that

of associating the emission with an active annulus on the polar cap. This is furthermore compatible with an $\mathbf{E} \times \mathbf{B}$ origin of subbeam circulation in B0943+10 (Deshpande & Rankin 1999, 2001; Asgekar & Deshpande 2001; Rankin, Suleymanova & Deshpande 2002) and is implicit in Ruderman & Sutherland's (1975; hereafter R&S) theory. It also follows from the recent aberration/retardation (hereafter A/R) delay analyses of B0329+54 by Malov & Suleymanova (1998; hereafter M&S) and G&G. To this end we can modify eq.(6) to include the parameter s, giving the fractional radius of the "active" annulus on the polar cap; see eq.(8) below (also Kijak & Gil 1997, 1998). The A/R studies argue that $s\approx 0.5$, implying that the h values given by eq.(6) are low by factors as large as 4.

$$h = 10P(\rho/s1.23^{\circ})^2 \text{ km}.$$
 (8)

Specifically, for B0329+54, M&S used 0.06-10.7-GHz observations and G&G 325- and 610-MHz observations to estimate their emission heights. Measuring the conal component spacings relative to the central (core) component (which is thought to be emitted at low altitude along the magnetic axis), and interpreting them as due to A/R delay, appropriate emission heights could be computed. Further, G&G reported that four pairs of conal components could be identified in the star's pulse sequences, which in turn exhibited progressive and symmetrical amounts of A/R delay. Our outer-cone analysis refers to their cone 3; whereas, M&S considered only this outer cone. The resulting conal emission heights at 103/111, 325 and 610 MHz are then some $945\pm55, 770\pm110,$ and 600±180 km, respectively, with respect to the core emission height. Using our separation measure, we find conal emission heights of 345 ± 188 , 229 ± 61 and 199 ± 32 km, respectively. Comparing these values using eq. (8), we find an average s of 0.56 ± 0.1 ; however, were the core emitted at a significant height, the former values would be increased by this amount and the resulting s values consequently decreased.

Almost a decade earlier, Blaskiewicz, Cordes, and Wasserman (1991; hereafter BCW) developed a method of estimating emission heights using the slight aberrational shift of the PA traverse relative to the profile center; and they then applied their

technique to a group of stars for which they had obtained exceedingly well measured polarization profiles—and a few of their pulsars are common to our sample. Then, more recently, von Hoensbroech & Xilouris (1997b) applied the same technique to another group of stars at somewhat different radio frequencies, and they also considered several stars of interest here.

Using the above results, three height values for B0301+19 were available at various frequencies, which could be compared with our (separation) height relation [Table 4; eq.(7)] via eq.(8)to determine the parameter s. Given our picture that a single active annulus on the stellar polar cap produces a cone of active field lines (which then radiate at different heights), it follows that s should be a (frequency-independent) constant for a given pulsar. The measured B0301+19 s values are 0.96 ± 0.3 , 1.3 ± 0.3 , and 0.23 ± 0.2 at 410, 1410 and 4850 MHz, respectively—giving a weighted average of 0.66 ± 0.15 . The five available values for B0525+21, 0.88 ± 0.3 , 0.66 ± 0.2 , $0.76\pm0.1, 0.41\pm0.15$ and 0.53 ± 0.12 at 430, 1410, 1418, 1710 and 4850 MHz, respectively, yield a weighted-average s of 0.63 ± 0.06 . For B1133+16, five further values, 0.85 ± 0.3 , 0.61 ± 0.1 , 0.82 ± 0.3 , 0.72 ± 0.1 and 0.62 ± 0.1 at the same frequencies, give 0.61 ± 0.06 . For B2045–16, only a 4850-MHz exists, 0.54 ± 0.1 . While there is considerable variation in the various individual s estimates, the weighted-average (outer cone) s values all fall within a narrow range between about 1/2 and 2/3.

We can now adjust the nominal 1-GHz, outercone, emission height of Paper VI in light of the above results, first by using the component-separation measure and second an appropriate s value. The effect of the first issue can be estimated by comparing the 3-db and separation height values at 1 GHz for A-group pulsars B0525+21, B1237+25 and B2045-16, and we find that the latter value is some 152 \pm 7 km (rather than the about 220-km value based on 3-db widths). The actual physical height is then s^{-2} times this value—or some 610 \pm 25 km if s is 0.5 or some 345 \pm 17 km if s is 0.67.

These outer-cone values are to be compared with the inner-cone emission heights of the group C pulsars, which are both smaller and virtually invariant. Here, comparing the 3-db versus the separation widths in Table 3, we find an average

ratio of some 0.89, which makes the nominal innercone emission height (using the separation measure) some 104 ± 6 km [as opposed to the Paper VI (3-db width) values of 130 km]. This nominal inner-cone height, when adjusted as above by s^{-2} , gives physical emission-height values between 415 and 235 km.

Finally, Wright (2002) has suggested that the outer-cone emission region is associated with the last open field lines, whereas the inner-cone region is along the "null" surface (Goldreich & Julian 1969; R&S) at $s=(2/3)^{3/4}=0.74$. If so, then the above arguments would suggest a physical 1-GHz, outer-cone emission height of 152 ± 7 km as well as an inner-cone height of 104 ± 6 km, scaled by s^{-2} , which is 191 ± 11 km. Note that this places in the 1-GHz inner-cone emission at a greater height than the 1-GHz outer-cone radiation, though RFM would reverse the situation at most lower frequencies.

Thus, we conclude that the 1-GHz emission heights $\rho_{\text{inner[outer]}}$ are 2-3 times larger than the respective 130[220]-km values of Paper VI, when referred to the component separation and adjusted for a "mean" $s{\sim}0.6$. If, however, inner- and outer-cone emission occurs along the "null" and "closed field" surfaces, then $\rho_{\text{inner[outer]}}$ could be some 150[190] km. While the $h_{\text{inner[outer]}}$ values appear independent of P, only the latter are independent of f, so that the two emission zones may overlap at high frequency—just as is observed in the "boxy" profiles of many double-cone M stars above 1 GHz.

9. Do the Component Widths Reflect the Conal Geometry?

We have seen above that, overall, the conal component widths exhibit a surprisingly constant spectral behavior. However, we also see some possibly significant variations, and we here explore whether these can be understood in terms of the overall conal emission geometry.

At any given frequency, we can use the 3-db width together with the component separation to compute the *radial* half width of the conal emission beam $\Delta \rho$ as

$$\Delta \rho = 2(\rho_{\rm 3db} - \rho_{\rm cs}),\tag{9}$$

where $\rho_{\rm cs}$ is the beam radius computed using the

separation and ρ_{3db} that from the 3-db widths.

Assuming both that h is a monotonic function of f and that a given component is associated with a specific (uniformly illuminated) bundle of field lines (perhaps because a cone of "emission columns" connects the stellar surface to the emission region along them) at a given height, we can ask whether the flaring of the (presumed) dipolar magnetic field is sufficient to be observed. In this geometry, the angle θ between the annular emission region and the magnetic axis can be expressed in terms of the height h as $\theta = 1.23^{\circ} s(h/10P)^{1/2}$. Then, we can find $\Delta\theta$, the radial (half-power) thickness of a thin annulus of "active" field lines at height h as

$$\Delta\theta = 2.45^{\circ} \Delta s (h/10P)^{1/2}$$
 (10)

Now we construct a model curve using eq.(10), where Δs is estimated at the highest available frequency—relative to a nominal s value of 0.6—by matching $\Delta \theta$ to $\Delta \rho$. Then, keeping Δs constant, $\Delta \theta$ can be calculated using eq.(10) where the height h is obtained from the component separation and using eq.(8) with s=0.6. On the other hand, $\Delta \rho$ can now be estimated using eq.(9) and this value compared with the corresponding dipolar flaring angle $\Delta \theta$ to study the deviations from a dipolar geometry.

In Figure 4 we plot both the $\Delta\theta$ model and the $\Delta \rho$ widths versus h for most of the outercone stars. (B0301+19 was omitted because of its strange "step", and B2020+28 and B2045-16 owing of their limited h ranges.) The curves indicate the dipole-flaring model $(\Delta \theta)$ bounded by $\Delta s \pm \sigma_{\Delta s}$, whereas the open circles $(\Delta \rho)$ show what flaring is seen in the observed fits. Both quantities entail errors in both h and ρ , which are included in the bounding curves $(\sigma_{\Delta s})$ or explicitly indicated. For most of the pulsars (including the excluded B2020+28 and 2045-16) the agreement between these flaring estimates is rather good. For B0329+54 the model works particular well, which in turn is compatible with the A/R analyses of M&S and G&G. Thus, any component narrowing at the highest frequencies can be understood as an angular narrowing in the radial (magnetic "zenith angle" θ) thickness of the emitting annulus (or cone) of field lines—though in some cases this may be compensated by the obliqueness of the sightline "cut" across the cone as β/ρ increases with fre-

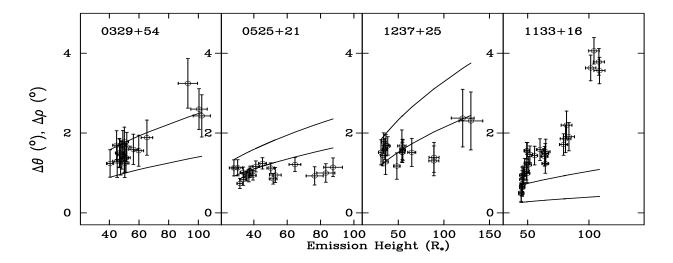


Fig. 4.— Conal beam width $\Delta \rho$ vs. emission height h for four pulsars with outer-cone component pairs. The pairs of curves represent the expected dipolar flaring $\Delta \theta$ of a conical emission beam corresponding to a polar cap annulus by Δs (see text). $\Delta \rho$ and $\Delta \theta$ have errors in both width and h which are shown explicitly or included in the bounding curves.

quency. Note that we have assumed here that s is independent of f. This is only true if the emission cone is uniformly illuminated at all frequencies, and scales in the way given by eq.(10). Deviations from either of the assumptions would lead to a frequency dependent s. This effect may be refected in Fig. 4, where the observed flaring (open circles) is consistently either lower or higher than the computed flaring (shaded) region. B1133+16 is the only star for which there is a significant discrepancy, possibly owing to its remarkably large value of β/ρ . Ignoring the lowest frequency (25 MHz) heights (where some scattering or instrumental effects may contribute), the width escalation at the lowest heights is much too steep to be dipole flaring; whereas, between 50 and 100 R_* , the s=0.6model works well.

In summary, assessment of whether these outer-cone beams flare in a dipolar manner depends critically on quality low frequency (large height) observations, which often remain problematic. Though the s=0.6 flaring model works well (except for B1133+16 as above), the B0525+21 analysis suggests a flaring which is less than dipolar. Higher quality observations at the lowest possible frequencies are needed to resolve the flaring issue.

10. Discussion and Conclusions

In the foregoing sections we have attempted an analysis of the conal component-pair dimension information for a set of 10 pulsars, the seven exemplars previously studied by Thorsett (1991) as well as three other prominent stars with very different characteristics. In carrying out our analysis, we have placed our focus on the angular scales of the (presumed circularly symmetric) conal emission beam pattern, not, as have most authors before us, on the longitude dimensions of the profiles. Computation of the beam sizes requires geometrical information which can perhaps yet only be estimated approximately; however, for most of these stars the very different approaches of Lyne & Manchester (1988) and one of us (Paper VI) give quite similar results.

In assessing what may be the most extensive set of well measured conal component-pair widths, we find that overall these widths vary little with frequency. We do observe some gentle narrowing at high frequencies in one or both of the components in some stars, a feature which was also observed by Sieber $et\ al\ (1975)$. We also find that some components appear to broaden at the very lowest frequencies, but here either instrumental effects or

scattering cannot yet be ruled out. It will be interesting, as coherent dedispersion techniques are more regularly applied to very low frequency observations over the next few years, to explore this question in further detail.

Because of these various sources of weak variation in the component widths, the profile-width measures which include them—the half-power (3-db) or 10%-width measures—we find, are more or less problematic indicators of the profile-scale variations. Therefore, our profile-scale analyses are based on the component-separation measure.

Our fitting, using the modified Thorsett relation eq.(5), of the conal beam radii ρ results in three strongly contrasting types of behavior. Four of the seven Thorsett stars exhibit continuously varying component separation, where, remarkably, the best-fit values of $\rho_{\rm o}$ are only 2–3-times larger than the angular radius of the polar cap $\rho_{\rm pc}$ and the index a takes values near –0.45. Three other stars have component separation values which seem to "saturate" at very high frequencies. Their best-fit values of $\rho_{\rm o}$ are 3–4 $\rho_{\rm pc}$ and the a values are substantially steeper. Then, in completely contrast to both these groups, we find three stars which exhibit almost no component-separation variation at all.

The first two behaviors are apparently exhibited by stars with outer-cone component pairs; whereas, the three examples of near constancy are all plausible or demonstrable examples of innercone component pairs. In regard to the first two groups, the A group can be well fitted by the "plasma frequency" index value of -1/3, but the B group cannot—and we have been unable to identify any geometrical circumstance that might account for the differences. We have also entertained whether higher-order contributions to the magnetic field configuration might account for them but, if so, why should we see two types of behavior rather than many? Certainly ten stars by no means provides an adequate statistical sample, but a preliminary examination of 9 further pulsars suggests that these too divide between the three groups.⁵

Furthermore, while the overall success of the modified Thorsett relation in fitting the profile-width spectra is satisfying, it remains merely an empirical relation. How then are we to understand the very necessity of the ρ_{\circ} term? And how could the index a of the Thorsett equation have physical implications similar to those attributed to simple power-laws of the same index?

A somewhat simpler picture emerged when we fitted the separation-determined h values as a direct function of f using eq.(7). The stars of both groups A and B could be fitted well with this relation, though the indices b for the latter group were substantially steeper. For the A group it was possible to impose an h_{\circ} value of 10 km (R_*) , without altering χ^2 very much. The real surprise, however, was that both groups could be fitted exceedingly well with an imposed index value of -2/3. These latter fits (see Table 4) have h_{\circ} values of between 5 and 15 times R_* .

Noting that emission heights computed from half-power widths in relation to the "last open field lines"—as in Paper VI—are not very physical, we suggest that more realistic values will come from the use of the component separation in relation to an annulus of "active" field lines about half way out on the polar cap, $s\sim0.5$. Such considerations lead to the conclusion that the 1-GHz outer-cone emission comes from a height of around 500–600 km (as opposed to 220 km in Paper VI), whereas the inner-cone emission stems from a height of some 400-500 km (c.f. 130 km). The first range agrees well with the several independent emissionheight determinations that are based on relativistic effects—which we summarized for those stars in our groups.

We have attempted to understand the component-width variations in terms of spectral changes in β/ρ and the height-dependent flaring of a dipolar magnetic field. The analysis seems largely consistent with such flaring (but depends critically on the difficult low frequency observations), and one pulsar suggests no flaring at all. Clearly, our study lends no simple support to the premise that the leading members of a component pair will be broadened by aberration (Ahmadi & Gangadhara 2002).

We are uncertain about how the strength and structure of the pulsar magnetic field might affect the radio emission heights. It may be that the

 $^{^5\}mathrm{These}$ objects, B0148–06, B0402–61, B0523+11, B0751+32, B1737+13, B1821+05, B1857–26, B2044+15 and B2319+60, constitute a promising short list for further study.

magnetic field configuration in the emission region will usually be nearly dipolar, and that closer to the surface there will always be non-dipolar effects [as the multipole field will not decay over the pulsar's lifetime (Mitra et al 1999)]. This will influence the gap heights in all vacuum-gap models—implicitly in the R&S theory and explicitly in later work as by, for instance, Muslimov & Tsygan (1992) or Gil & Mitra (2001). (It will also complicate interpretation of the s parameter.) Further, non-dipolar fields will increase the binding energy of the ions on the stellar surface (Abrahams & Shapiro 1991, Gil & Mitra 2001), which is by far the most problematic issue in forming gaps in pulsars.

In several theories we might expect the gap height to have an inverse relationship with the Bfield strength, and thus, the emission region which is argued to be proportional to the gap height, may start at a lower altitude in pulsars with stronger fields; however, here the field in question must be the total field in the gap region, including both the dipolar and non-dipolar contributions. We note that two of the A-group stars have (spindowndetermined, meaning dipolar?) field strengths of $\sim 10^{13}$ Gauss, while none of the B- or C-group star fields are this high (see Table 1). That many interpulsars seem to emit from both poles almost equally is also worth remembering, in that it implies that gaps can be formed above polar caps of either sense (with accelerated charges of either sign?)—and perhaps the two gap senses give rise to the two RFM types (A and B) observed above.

A major impetus for this work was that of trying to forge a better overall understanding of "RFM mapping" to facilitate its physical interpretation. The summary of Xilouris et al is very useful, but we have been unable to locate any full theoretical discussion of RFM [excepting that of Barnard & Arons (1986), which predicts no RFM at all]. Returning to R&S, we find that those stars which exhibit RFM—that is, our groups A and B—can be fitted with an index of -2/3, which they associated with curvature radiation. Of course, our fitting does not determine this index, as it is highly correlated with the other two parameters; however, it is significant, we believe, that an index of -2/3 can be imposed on both the group A and B stars without any serious degradation of χ^2 .

If the index b in the modified Thorsett rela-

tion can be interpreted straightforwardly in R&S terms, then this dependence represents an underlying physical situation in which particles of a particular γ radiate at different heights because the field-line curvature ρ_c and the plasma frequency ω_p in turn vary systematically with height. Thus, if the magnetic field is dipolar in the emission region, perhaps R&S's eq.(64) can meaningfully be evaluated to obtain the controlling quantity $\gamma_{\rm max}$. Other theories, however, may view this circumstance very differently, but must find a natural explanation for this specific RFM phenomenon.

A nearly opposite circumstance is observed in stars with no RFM. How can broad-band emission at a single, fixed height be understood?—a situation which R&S have not at all addressed. Apparently, this inner-cone "no-RFM" situation is as general as the outer-cone RFM, and indeed both situations commonly appear in those stars with both inner- and outer-cone emission. This dichotomy is suggestive of the wave-mode propagation model first advanced in comprehensive detail by Barnard & Arons (1986). Though not free of problems, this model addresses the effects of birefringence in the pulsar magnetosphere, such that one propagating wave-mode escapes the magnetosphere at different heights mimicking the usual (outer cone) RFM behavior, whereas the other mode can probably escape from a fixed height with results similar to the "no-RFM" (inner cone) phenomenon. This said, it is not clear that inner and outer cones exhibit the systematic polarization differences which might be expected of distinct propagating wave modes—and, birefringence could also be involved in the angular shifts seen between the two polarization modes (Rankin & Ramachandran 2002). So, while we cannot be sure that propagation effects are responsible for these dramatic differences, we are sympathetic to the possibility, and it remains possible that a more flexible propagation model such as Petrova's (2001 and the references cited therein) could account for the systematics of both beaming and polarization.

So, in conclusion, our results seem nominally compatible with the picture that conal beams are produced by a system of subbeams circulating around the magnetic axis some halfway out on the polar cap, which in turn are produced, perhaps, by excitation in "vaccum gaps" and radiate by a mechanism wherein the plasma frequency de-

termines the emission height. Nothing, however, in our analysis, has demonstrated these specific physical circumstances.

We thank Steve Thorsett for generously sharing his notes and the profile measurements used in the preparation of his earlier paper. We also thank Michael Kramer both for his insightful comments on our manuscript as well as for the use of his Gaussian-fitting programs, and Yashwant Gupta for providing several needed profiles using the GMRT. Several profiles were obtained from the extremely useful pulsar database of the European Pulsar Network maintained by Max-Planck Institut für Radioastronimie. We also learned much from discussions and comments on early versions of the manuscript from Jim Cordes, Jan Gil, Aris Karastergiou, George Melikidze, R. Ramachandran, Mal Ruderman, C. S. Shukre, Axel Jessner and Steve Thorsett. Portions of this work were carried out under US National Science Foundation (NSF) Grants INT 93-21974 and AST 99-87654 as well as under a visitor grant from the Nederlandse Organisatie voor Wetenschappelijk Onderzoek. Arecibo Observatory is operated by Cornell University under contract to the US NSF.

REFERENCES

- Ahmadi, P., & Gangadhara, R. T. 2002, ApJ, 566, 365
- Arzoumanian, Z., Nice, D.J., Taylor, J.H. & Thorsett, S.E., 1994, ApJ, 422, 671
- Asgekar, A. & Deshpande, A. A. 2001, MNRAS, 326, 1249
- Backer, D. C. 1976, ApJ, 209, 895
- Barnard, J. J. & Arons, J., 1986, ApJ, 302, 138
- Blaskiewicz, M., Cordes, J. M., & Wasserman, I. 1991, ApJ, 370, 643 (BCW)
- Cordes, J. M. 1978, ApJ, 222, 1006
- Deshpande, A. A. & Rankin, J. M. 1999, ApJ, 524, 1008
- Deshpande, A. A. & Rankin, J. M. 1999, MNRAS, 322, 438

- Gangadhara, R. T. & Gupta, Y. 2001, preprint (G&G)
- Gil, J. A. 1981, Acta Phys. Polonicae, B12, 1081
- Gil, J. A., Kijak, J., & Seiradakis, J. M. 1993, A&A, 272, 268
- Gil, J., & Mitra, D. 2001, ApJ, 550, 383
- Goldreich, P. & Julian, W. H. 1969, ApJ, 157, 869.
- Gould, D. M. & Lyne, A. G. 1998, MNRAS, 301, 235
- Hankins, T. H., Rankin, J. M., & Eilek, J. A., 2002, in preparation
- von Hoensbroech, A., & Xilouris, K. M. 1997a, A&AS, 126, 121
- von Hoensbroech, A., & Xilouris, K. M. 1997b, A&A, 324, 981
- Izvekova, V. A., Kuz'min, A. D., Lyne, A. G., Shitov, Yu. P. & Smith, G. F., 1993, MNRAS, 261, 865
- Kardashev, N. S., Nikolaev, N. Ya., Novikov, A. Yu., Popov, M. V., Soglasnov, V. A., Kuz'min, A. D., Smirnova, T. V., Sieber, W., & Wielebinski, R. 1986, A&A, 163, 114
- Kijak, J., & Gil, J., 1997, MNRAS, 288, 631
- Kijak, J., & Gil, J., 1998, MNRAS, 299, 855
- Kijak, J., Kramer, M., Wielebinski, R. & Jessner, A., 1998, A&AS, 127, 153
- Kijak, J., Kramer, M., Wielebinski, R. & Jessner, A., 1997, A&A, 318L, 63
- Komesaroff, M. M. 1970, Nature, 225, 612
- Komesaroff, M. M., Morris, D., & Cooke, D. J. 1970, Astrophysical Letters, 5, 37
- Kramer, M. 1994, A&AS, 107, 527
- Kramer, M., Wielebinski, R., Jessner, A., Gil, J. A., & Seiradakis, J. M. 1994, A&AS, 107, 515
- Kramer, M., Xilouris, K.M., Jessner, A., Lorimer, D.R., Wielebinski, R. & Lyne, A.G., 1997a, A&A, 322, 846

- Kramer, M., Jessner, A., Doroshenko, O. & Wielebinski, R., 1997b, ApJ., 489, 364
- Kuz'min, A.D. & Izvekova, V.A., 1996, AstL, 22, 394
- Kuz'min, A.D. & Losovskii, B.Y., 1999, Astronomy Reports, 43, 288
- Lyne, A. G., Smith, F. G. & Graham, D. A. 1971, MNRAS, 153, 337
- Lyne, A. G., & Manchester, R. N. 1988, MNRAS, 234, 477
- Malofeev, V. M. 1994, A&A, 285, 201
- Malofeev, V. M. 2001, preprint
- Malov, I. F., & Suleymanova, S. A. 1998, Astronomy Reports, 42, 388 (M&S)
- Maron, O., Kijak, J., Kramer, M. & Wielebinski, R., 2000, A&AS, 147, 195.
- McCulloch, P. M., Hamilton, P. A., & Manchester, R. N. (1982), preprint
- McKinnon, M. M. 1997, ApJ, 475, 763.
- Mitra, D., & Deshpande, A. A. 1999, A&A, 343, 906
- Mitra, D. 2002, private communication
- Mitra, D., Konar, S., & Bhattacharaya, D., 1999, MNRAS, 307, 459
- Muslimov, A. G., & Tsygan, A. I. 1992, MNRAS, 255,61
- Petrova, S. A. 2001, A&A, 378, 883.
- Phillips, J. A. 1992, ApJ, 385, 282
- Press, W. H., Flannery, B. P., Teukolsky, S. A., & Vetterling, W. T. 1986, *Numberical Recipes* (Cambridge Univ. Press; Cambridge)
- Prószynski, M. & Wolszczan, A., 1986, ApJ,307, 540
- Radhakrishnan, V., & Cooke, D. J. 1969, Astrophys. Lett., 3, 225
- Ramachandran, R., Rankin, J. M., Stappers, B. W., Kouwenhoven, M. L. A., & van Leeuwen, A. G. L. 2002, A&A, 381, 993

- Ramachandran, R., Rankin, J, M, & Deshpande, A. A. 2002, ApJ, preprint
- Rankin, J. M. 1983a, ApJ, 274, 333 (Paper I)
- Rankin, J. M. 1983b, ApJ, 274, 359 (Paper II)
- Rankin, J. M. 1988, ApJ, 325, 314
- Rankin, J. M. 1990, ApJ, 352, 247 (Paper IV)
- Rankin, J. M. 1993a, ApJ, 405, 285 (Paper VIa)
- Rankin, J. M. 1993b, ApJS, 85, 145 (Paper VIb)
- Rankin, J. M. & Rathnasree, N. 1997, Journal of Astrophysics & Astronomy, 18, 91
- Rankin, J. M., Suleymanova, S. A. & Deshpande, A. A 2001, preprint
- Rankin, J. M. & Ramachandran, R., 2002, preprint
- Ruderman, M. A., & Sutherland, P. G. 1975, ApJ, 196, 51
- Seiradakis, J.H., Gil, J.A., Graham, D.A., Jessner, A., Kramer, M., Malofeev, V.M., Sieber, W. & Wielebinski, R., 1995, A&AS, 111, 205
- Sieber, W., Reinecke, R., & Wielebinski 1983, A&A, 38, 169
- Slee, O. B., Bobra, A. D. & Alurkar, S. K. 1987, Australian Journal Physics, 40, 557
- Thorsett, S. E. 1991, ApJ, 377, 263
- Weisberg, J. M., Cordes, J. M., Lundgren, S. C., Dawson, B. R., Despotes, J. T., Morgan, J. J., Weitz, K. A., Zink, E. C. & Backer, D. C., 1999, ApJS, 121, 171
- Wright, G. A. E. 2002, MNRAS, preprint
- Xilouris, K. M., Kramer, M., Jessner, A., Wielebinski, R., & Timofeev, M. 1996, A&A, 309, 481

This 2-column preprint was prepared with the AAS IATEX macros v5.0.

 ${\it Table~2}$ Fit Parameters for the Leading and Trailing Components Widths.

Pulsar B-/	Freq-range	K	ζ	χ^2	Μ	References
Component	(GHz)	$(^{\circ}/\mathrm{GHz}^{\zeta})$	· ·			
0901 + 10 T	0.1.4.0	9.711.6	0.00 0.00	1.00	10	1.0.0
0301+19 I II	0.1-4.9	3.7 ± 1.6	0.20 ± 0.02	1.20	19	1,2,3
II I	0.1-4.9	3.9 ± 1.0	0.04 ± 0.02	$1.00 \\ 0.16$	19	4,6,9
	0.1 - 0.5	2.7 ± 0.1	-0.05 ± 0.09		9	10,11
II	0.1-0.5	4.6 ± 0.1	0.14 ± 0.09	1.60	9	14
I	0.6-4.9	4.1 ± 0.1	0.09 ± 0.05	1.01	10	
II	0.6 – 4.9	4.1 ± 0.2	0.04 ± 0.06	0.60	10	
0329+54 I	0.1 – 10.5	2.9 ± 0.01	0.01 ± 0.03	0.4	19	2,4,5
II	0.1 - 10.5	3.2 ± 0.02	-0.21 ± 0.02	1.0	19	7,8,9
II	0.2 - 10.5	3.0 ± 0.02	-0.12 ± 0.05	0.5	16	10.11
	0.2 10.0	0.0±0.02	0.12 ± 0.00	0.0	10	10.11
0525 + 21 I	0.1 – 4.9	2.7 ± 0.01	-0.06 ± 0.03	0.76	19	2,3,4,9
II	0.1 – 4.9	2.8 ± 0.01	-0.04 ± 0.03	1.69	19	10,11,14
						, ,
1133 + 16 I	0.02 – 10.5	2.1 ± 0.03	-0.16 ± 0.01	2.7	31	2,3,9
II	0.02 – 10.5	$3.2 {\pm} 0.01$	-0.13 ± 0.01	5.5	31	$4,\!6,\!7$
I	0.04 – 10.5	2.2 ± 0.01	-0.06 ± 0.02	1.14	26	10,11
II	0.04 – 10.5	3.3 ± 0.01	-0.09 ± 0.02	5.00	26	
1237 + 25 I	0.04 – 4.9	1.7 ± 0.02	-0.005 ± 0.03	1.1	18	1,2,3,4
II	0.04 – 4.9	$2.2 {\pm} 0.01$	0.006 ± 0.02	2.1	18	9,10,11,14
2020+28 I	0.1 – 10.5	$3.4 {\pm} 0.01$	-0.04 ± 0.03	4.0	15	2,3,9
II	0.1 – 10.5	2.7 ± 0.01	-0.13 ± 0.03	1.8	15	$4,\!10,\!11,\!12$
2045–16 I	0.1 – 4.9	2.9 ± 0.01	-0.14 ± 0.04	1.5	12	$2,\!6,\!4$
II	0.1 – 4.9	2.6 ± 0.01	-0.19 ± 0.04	1.5	12	$10,\!11,\!13$
0834+06 I	0.04 – 4.9	2.1 ± 0.02	$0.04{\pm}0.02$	1.5	17	3
0034+00 I	0.04 - 4.9 $0.04 - 4.9$	2.1 ± 0.02 2.9 ± 0.1	-0.04 ± 0.02 -0.01 ± 0.01	$\frac{1.5}{3.7}$	17	3
11	0.04-4.9	2.9±0.1	-0.01±0.01	3.1	11	
1604-00 I	0.04 – 4.9	2.1 ± 0.3	-0.09 ± 0.05	3.0	6	3
II	0.04 - 4.9	1.4 ± 0.2	-0.15 ± 0.05	1.5	6	-
1919+21 I	0.04 – 4.9	$3.1 {\pm} 0.1$	0.10 ± 0.04	1.1	15	3
I	0.4 – 4.9	$3.3 {\pm} 0.02$	-0.10 ± 0.09	3.0	11	
II	0.04 – 4.9	$3.2 {\pm} 0.01$	-0.01 ± 0.03	1.0	15	
II	0.4 – 4.9	$3.2 {\pm} 0.01$	-0.11 ± 0.05	0.4	11	

REFERENCES.— (1) Arzoumanian et al 1994; (2) Gould & Lyne 1998; (3) Hankins, Eilek & Rankin 2002; (4) Hoensbroech & Xilouris 1997a: (5) Hoensbroech & Xilouris 1997b; (6) Kijak et al 1997; (7) Kramer et al 1997; (8) Kuz'min & Izvekova 1996; (9) Kuz'min & Losovskii 1999; (10) Seiradakis et al 1995; (11) Thorsett 1991; (12) Gupta 2001 (private communication); (13) McCulloch et al 1982; (14) Mitra 2002 (Unpublished test beservations at 8.35 GHz using Effelsberg Radio Telescope, private communication.)

 $\begin{tabular}{ll} TABLE 3 \\ FIT PARAMETERS FOR THE CONAL BEAM RADII. \end{tabular}$

Pulsar (B-)	$\rho_{\circ}(^{\circ})$	f _o (GHz)	a	C_{ij} (%)	χ^2	M
Component Se	eparation —	Group A				
0301+19	2.29 ± 0.2	2.1 ± 0.9	-0.47 ± 0.06	+92,-96,-99	0.5	29
0501 + 19 0525 + 21	1.70 ± 0.2	0.4 ± 0.01	-0.40 ± 0.08	+93,-97,-99	0.5	19
1237 + 25	2.98 ± 0.2	1.1 ± 0.2	-0.45 ± 0.05	+90,-95,-98	0.5	$\frac{13}{42}$
2045-16	2.72 ± 0.2	0.4 ± 0.05	-0.43 ± 0.03 -0.42 ± 0.01	+93,-97,-99	1.0	32
0301+19	1.040	48 ± 5	-0.26 ± 0.01	-98.7	0.9	29
0525 + 21	0.633	30 ± 10	-0.18 ± 0.01	-98.8	1.1	19
1237 + 25	$\boldsymbol{1.042}$	390 ± 100	-0.19 ± 0.01	-98.5	1.1	42
2045 - 16	$\boldsymbol{0.875}$	552 ± 200	-0.15 ± 0.01	-98.7	1.4	32
0301 + 19	1.040	19.5 ± 0.3	-1/3		2.2	29
0525 + 21	0.633	5 ± 0.5	-1/3	_	20	19
1237 + 25	1.042	20 ± 0.3	-1/3		13	42
2045 - 16	0.875	13 ± 0.5	-1/3	_	28	32
0301 + 19	1.59 ± 0.3	10.2 ± 1.2	-1/3	-94.3		29
	1.59 ± 0.3 1.5 ± 0.1	0.7 ± 0.3	,	-94.3 -94.3	$0.7 \\ 0.6$	19
0525+21 $1237+25$	1.3 ± 0.1 2.4 ± 0.3	0.7 ± 0.5 3.9 ± 0.5	-1/3	-94.5 -93.7	0.6	42
2045-16	2.4 ± 0.3 2.34 ± 0.3	3.9 ± 0.3 1.2 ± 0.4	-1/3	-93.1 -93.9	1.1	32
2045-10	2.34 ± 0.3	1.2 ± 0.4	-1/3	-93.9	1.1	32
Component Se	-	-				
0329 + 54	6.0 ± 0.1	0.259 ± 0.045	-1.07 ± 0.17	+83,-88,-99	0.9	19
1133 + 16	4.4 ± 0.02	0.121 ± 0.033	-0.55 ± 0.03	+74,-83,-97	1.1	62
2020 + 28	8.7 ± 0.1	0.165 ± 0.080	-0.89 ± 0.11	+76, -75, -99	1.0	35
0329 + 54	4.6 ± 0.3	3.4 ± 1.0	-1/3	-90.1	1.6	19
1133 + 16	3.9 ± 0.2	0.4 ± 0.3	-1/3	-86.0	5.6	62
2020+28	8.3 ± 0.3	0.381 ± 1.4	-1/3	-91.0	3.0	35
Half-power Wi	idths — Gro	up A				
0301 + 19	1.040	$1.8 \pm 0.5 \times 10^3$	-0.185 ± 0.03	-98.7	1.3	29
0525 + 21	0.633	262 ± 100	-0.15 ± 0.01	-98.7	1.0	19
1237 + 25	$\boldsymbol{1.042}$	$9.6 \pm 5.0 \times 10^3$	-0.15 ± 0.02	-98.3	1.6	18
2045–16	0.875	$5.0 \pm 3.0 \times 10^3$	-0.14 ± 0.02	-99.3	1.2	12
Half-power Wi	idths — Gro	up B				
0329 + 54	6.4 ± 0.4	0.359 ± 0.085	-1.00 ± 0.22	+83,-88,-99	0.7	19
1133+16	4.6 ± 0.2	0.310 ± 0.100	-0.51 ± 0.30	+75,-84,-98	4.0	30
2020+28	9.4 ± 0.3	0.205 ± 0.160	-0.88 ± 0.15	+85,-89,-99	0.6	16
10% Widths $-$	- Group A					
0301+19	1.040	$2.6\pm0.4\times10^5$	-0.13 ± 0.02	-99.7	0.6	24
0525+21	0.633	$2.9 \pm 1.2 \times 10^3$	-0.13 ± 0.02 -0.13 ± 0.02	-99.1	1.1	17
1237+25	1.042	$1.6 \pm 1.5 \times 10^{3}$	-0.13 ± 0.02 -0.13 ± 0.02	-99.3	0.5	20
2045–16	0.875	$1.0 \pm 1.0 \times 10^{5}$ $1.0 \pm 1.0 \times 10^{5}$	-0.13 ± 0.02 -0.12 ± 0.03	-99.5	$0.5 \\ 0.5$	8
10% Widths –	- Group B					
0329 + 54	7.4 ± 0.4	0.401 ± 0.200	-1.12 ± 0.30	+75,-78,-99	0.5	18
1133+16	5.3 ± 0.2	0.350 ± 0.080	-0.55 ± 0.02	+93,-98,-98	3.5	36
2020+28	9.9 ± 0.2	0.544 ± 0.350	-0.83 ± 0.10	+90,-94,-99	0.7	15
2020 20	0.0 ± 0.1	J.J.I U.J.U	0.00-0.10	100, 04, 00	0.1	10

Table 3—Continued

Pulsar (B–)	$\rho_{\circ}(^{\circ})$	$f_{\circ}~(\mathrm{GHz})$	a	C_{ij} (%)	χ^2	M			
Component Se	paration —	- Group C							
-	•	Group C			0.0	17			
0834 + 06	3.6 ± 0.3	_			0.2	17			
1604-00	6.1 ± 0.4				0.3	6			
1919 + 21	3.3 ± 0.2	_	_	_	0.2	15			
Half-power Widths — Group C									
0834 + 06	3.9 ± 0.3	_	_	_	0.1	17			
1604-00	6.8 ± 0.4				0.1	6			
1919 + 21	3.8 ± 0.3	_	_	_	0.8	15			
10% Widths — Group C									
0834 + 06	4.2 ± 0.3		_	_	0.3	16			
1604-00	8.1 ± 0.3		_	_	1.6	6			
1919 + 21	4.2 ± 0.5	_		_	0.1	15			

 $\begin{tabular}{ll} Table 4 \\ Fit Parameters for the Emission Heights. \end{tabular}$

Pulsar (B-)	$\mathrm{h}_{\diamond}(\mathrm{Km})$	f _h (GHz)	b	C_{ij} (%)	χ^2	\overline{M}			
Component Separation — Group A									
0301+19	57.7 ± 7.0	365 ± 50	-0.69 ± 0.07	+89,-93,-99	0.5	29			
0525+21	81.0 ± 12.8	$2.1 \pm 1.0 \times 10^3$	-0.54 ± 0.08	+91,-95,-99	0.5	19			
1237 + 25	91.9 ± 8.1	779 ± 100	-0.61 ± 0.05	+87,-92,-99	0.5	42			
2045–16	104 ± 11.0	$1.8 \pm 0.9 \times 10^3$	-0.54 ± 0.08	+91,-95,-99	1.0	32			
0301 + 19	10	$8.7 \pm 5.0 \times 10^{3}$	-0.42 ± 0.02	98.9	1.1	29			
0525 + 21	10	$2.2 \pm 0.7 \times 10^7$	-0.29 ± 0.03	98.9	1.1	19			
1237 + 25	10	$1.4 \pm 0.6 \times 10^7$	-0.30 ± 0.02	98.6	1.2	42			
2045 – 16	10	$1.7 \pm 0.8 \times 10^9$	-0.24 ± 0.02	98.8	1.4	32			
0301 + 19	54.7 ± 5.0	$5.0 \pm 2.0 \times 10^3$	-2/3	-81.0	0.5	29			
0525 + 21	95.2 ± 7.0	360 ± 50	-2/3	-79.8	0.6	19			
1237 + 25	98.0 ± 10.0	380 ± 200	-2/3	-78.8	0.5	42			
2045 – 16	117.1 ± 10.0	320 ± 50	-2/3	-78.7	1.0	32			
Component Separation — Group B									
0329 + 54	158.7 ± 10.0	43.8 ± 10.0	-0.87 ± 0.17	+80,-84,-99	0.5	19			
1133 + 16	158.9 ± 10.0	29.9 ± 5.03	-0.76 ± 0.03	+70,-79,-98	0.6	62			
2020+28	178.6 ± 10.0	4.3 ± 1.0	-1.10 ± 0.11	+73,-77,-99	0.8	35			
0329 + 54	147.3 ± 10.0	302 ± 50	-2/3	-69.0	0.6	19			
1133 + 16	153.6 ± 10.0	85.5 ± 10.0	-2/3	-64.0	0.9	62			
2020+28	173.5 ± 5.0	45.6 ± 5.0	-2/3	-73.0	1.2	35			